



On the pore forming mechanism of Upsalite, a micro- and mesoporous magnesium carbonate



Sara Frykstrand, Johan Forsgren, Albert Mihranyan, Maria Strømme*

Division for Nanotechnology and Functional Materials, Department of Engineering Sciences, The Ångström Laboratory, Uppsala University, Box 534, SE-751 21 Uppsala, Sweden

ARTICLE INFO

Article history:

Received 3 July 2013

Received in revised form 6 December 2013

Accepted 11 December 2013

Available online 19 December 2013

Keywords:

Pore forming mechanism

Surfactant-free

In situ gas template

Mesoporous

Magnesium carbonate

ABSTRACT

This work analyzes the pore forming mechanism and stability of Upsalite; an extraordinary moisture absorbing, high-surface area magnesium carbonate powder synthesised without the use of surfactants as pore forming agents. The pores in Upsalite were found to be created in a two-step process where the first step includes the formation of micropores by solvent evaporation and release of physically bound carbon dioxide, acting as an *in situ* pore-forming template. In the second step, the micropores expand to mesopores due to partial decomposition of organic groups on the surface of the pore walls when the material is stored in air at moderate temperatures (70 °C). The resulting material has a narrow pore size distribution centered at 5 nm, and the amorphous structure is stable upon storage in a humid atmosphere.

It was further shown that calcination at temperatures above 250 °C is required for complete removal of the organic surface groups in Upsalite. Prior to calcination, the organic groups present in the material act as barriers hindering water to induce crystallization of the bulk material. After calcination, however, Upsalite crystallizes into nesquehonite when stored at 100% relative humidity for several days. The results presented herein are expected to be useful for the development of novel surfactant-free synthesis routes of porous materials as well as for the understanding of the long-term performance of such materials.

© 2013 The Authors. Published by Elsevier Inc. This is an open access article under the CC BY-NC-ND license (<http://creativecommons.org/licenses/by-nc-nd/3.0/>).

1. Introduction

Micro- and mesoporous inorganic solids having large internal surface areas and controllable pore size distributions are subjects for extensive research, especially with regard to the many potential applications for this type of materials, e.g. as catalysis and sorption media [1–6], in regeneration of bone tissue [7,8], as vaccine adjuvants [9,10], drug delivery vehicles [11,12] as well as in cosmetics [13]. Since ordered mesoporous silica entered the scene in the early 1990's, the concept of using surfactants as pore forming templates has been widely used in order to develop a variety of ordered mesoporous materials [14–17]. Although there are examples in the literature where ordered mesoporous silica has been synthesized without the use of surfactants [18], the surfactant route is still the most common one. However, while the use of surfactants offers many advantages like the possibility to precisely control the pore size, shape, and connectivity as well as the particle shape it also comes with some disadvantages such as

the need for subsequent removal of the organic surfactants after synthesis of the inorganic matrix, which involves the use of either high temperatures or chemicals that add time, costs and increase the environmental burden of the production process. The use of surfactants also rules out the possibility of *in situ* loading the pores with active agents (*i.e.* pharmaceutical, cosmetic, agricultural compounds and the likes) during synthesis unless the agent *per se* is amphiphilic [19,20].

Further, in applications like adsorption or catalysis it is desirable to have materials that exhibit a disordered interconnected three dimensional network of uniform pores where the internal volume is more accessible to external components rather than a unidirectional pore system like those often present in ordered mesoporous material synthesized using ordinary template-based methods [4,21,22].

One of the driving forces for the development of new porous material is to increase the pore size to permit the penetration of large molecules into the porous framework [23–25]. Hence avoiding the use of surfactants in the synthesis and still form a mesoporous materials may be desirable, not only because it maintains the production costs low and has less environmental impact

* Corresponding author. Tel.: +46184717231

E-mail address: maria.stromme@angstrom.uu.se (M. Strømme).

for an up-scaled production process, but also since it offers the possibility of *in situ* loading of active, non-template forming agents. The latter concept has previously been demonstrated for mesoporous calcium carbonate where the poorly soluble pharmaceutical substance celecoxib was incorporated *in situ* during material's synthesis with the aim to conserve the amorphous state of the incorporated substance and hence increase the solubility of the same [26].

We recently reported on the synthesis of a porous and amorphous magnesium carbonate, referred to as Upsalite, with a narrow pore size distribution centered around 3 nm and the largest specific surface area measured for an alkaline earth metal carbonate; $\sim 800 \text{ m}^2/\text{g}$ [27]. The material was synthesized in a low-temperature process without using surfactants where magnesium oxide and methanol were reacted together with carbon dioxide under pressure. The magnesium carbonate was formed upon decomposition of the reaction product when heat-treated at 70 °C, which led to solidification of the material. The moisture sorption of Upsalite was found to be featured by a unique set of properties including an adsorption capacity $\sim 50\%$ larger than that of the hygroscopic zeolite-Y at low relative humidities making the material highly interesting in humidity control applications.

In the present work we perform a detailed investigation of the pore formation mechanism and analyze the structural stability of Upsalite. We demonstrate that micropores are formed in the as-synthesized material as a consequence of the intermediate products in the synthesis acting as foaming agents releasing carbon dioxide and methanol during decomposition. The evolution of carbon dioxide gas causes swelling of the gel phase before it solidifies and dries, resulting in the formation of micropores. When stored in air at moderate temperatures, these micropores expand into mesopores with a pore width of around 5 nm through partial decomposition of methoxyl and hydroxyl groups still present in the material. The pore size distribution in the finally mesoporous material is narrow compared to other dried magnesium carbonate-based porous gels that exhibit a broader size distribution of pores over the entire mesoporous region [28].

2. Experimental section

2.1. Materials

Magnesium oxide (MgO, >99%) and methanol (>99.8%), were purchased from Sigma–Aldrich. Carbon dioxide (CO₂, N48) was purchased from Air Liquid. All reagents were used without further purification.

2.2. Synthesis

Upsalite was synthesized as described earlier [27], but with the exception that the solidification/drying time was reduced from three to two days. Briefly, 8 g magnesium oxide and 120 ml methanol were reacted in a reaction vessel under carbon dioxide pressure with an initial pressure of 3 bar and a temperature of 50 °C. After 3 h the heating was turned off and the pressure was lowered. The suspension was left in the reactor until a gel had formed after which the reactor was depressurized and the gel was put in a 70 °C furnace to solidify and dry for 2 days. The obtained material was analyzed immediately after the two day drying period (referred to as the as-synthesized material) and also after being stored at 70 °C in air for one and three months. After three months of storage, a part of the material was calcined at 300 °C under nitrogen gas flow using a 10 h ramp time from room temperature and a 10 h hold time at 300 °C (referred to as the calcined material) before analyzed.

2.3. Characterization

Nitrogen sorption measurements were carried out at 77 K using an ASAP 2020 from Micromeritics. The samples were degassed at 95 °C under vacuum for 10 h prior to analysis with a vacuum set point of 10 $\mu\text{m Hg}$. The specific surface area (SSA) was determined by applying the Brunauer–Emmet–Teller (BET) equation [29] to the relative pressure range 0.05–0.30 of the adsorption branch of the isotherm. The micropore volume was determined by the Dubinin–Asthakov (D–A) equation [30] in the appropriate pressure region for adsorption into micropores. The BET and D–A calculations were performed with the ASAP 2020 V3.04 software from micromeritics. The pore size distribution was determined using the DFT method carried out with the DFT plus software from micromeritics using the model for nitrogen adsorption at 77 K for slit-shape geometry with no-negative regularization and high smoothing ($\lambda = 0.02000$). The standard deviation of the DFT fit was between 1.1 cm^3/g and 2.5 cm^3/g STP for the recorded isotherms.

Thermal decomposition products from Upsalite were characterized with a thermal gravimetric analysis (TGA)/fourier transform infrared spectroscopy (FTIR) coupled instrument for evolved gas analysis (EGA). For this a TGA Q500 instrument coupled to a FTIR Nicolet iS10, both from ThermoScientific, with a TGA/FTIR interface, was used. The temperature of the gas tube between TGA and FTIR was set to 220 °C, constant temperature. The analysis was carried out in a nitrogen atmosphere with the sample placed in a platinum cup with a sample size of approximately 17 mg. The sample was heated from 30 °C to 700 °C with a heating ramp of 10 °C/min.

X-ray diffraction (XRD) analysis was performed with a Bruker D8 TwinTwin instrument using Cu–K _{α} radiation. Samples were ground and put on a silicon zero background sample holder prior to analysis. The instrument was set to operate at 45 kV and 40 mA. Analyses of the diffractogram were performed using the software EVA V2.0 from Bruker.

FTIR was performed with a Bruker Tensor27 instrument using a platinum ATR diamond cell. A background scan was recorded prior to the measurement and subtracted from the sample spectrum, 100 scans were signal-averaged for each spectrum.

HRTEM images were taken with a JEOL-3010 microscope, operating at 300 kV (Cs 0.6 mm, resolution 1.7 Å). Images were recorded using a CCD camera (model Keen View, SIS analysis, size 1024 \times 1024, pixel size 23.5 \times 23.5 μm) at 30000–100000 \times magnification using low-dose conditions on as-crushed samples.

The sample stored in air at 70 °C for three months was used for the XRD, FTIR, TEM and EGA analyses.

3. Results and discussion

The synthesis resulted in formation of a white material consisting of centimeter-sized grains with irregular shape, Fig. 1a. In Fig. 1b a TEM image of the Upsalite can be seen, showing dark contrast due to the structure of the material. The XRD pattern of the obtained material was consistent with previously recorded XRD patterns for Upsalite [27] indicating an amorphous nature of the material with traces of residual unreacted magnesium oxide, Fig 2a. No changes in the XRD pattern could be observed for the material after storage at 70 °C for three months or after calcination. TGA analysis also confirmed that the MgO content in the material remained unchanged throughout the study and hence proves that no further reaction involving the oxide component occurred after the gel had solidified. The FTIR spectrum of the material, Fig. 2b, exhibited the characteristic absorption bands for the carbonate group at ~ 1440 , ~ 1100 and $\sim 850 \text{ cm}^{-1}$ [31]. Further, the FTIR

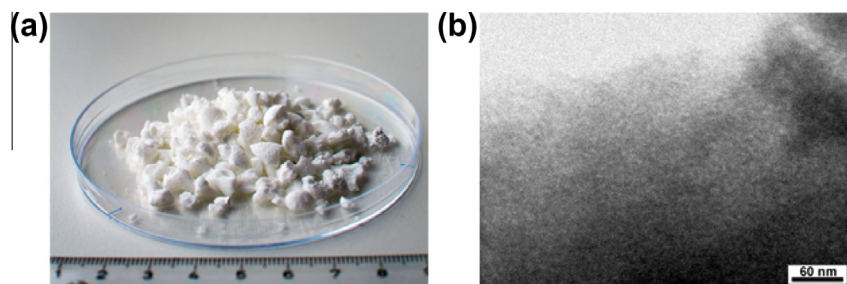


Fig. 1. (a) Image of as-synthesized Upsalite, (b) TEM image of Upsalite stored for three months at 70 °C, the magnesium carbonate appears in dark contrast due to the structure of the material.

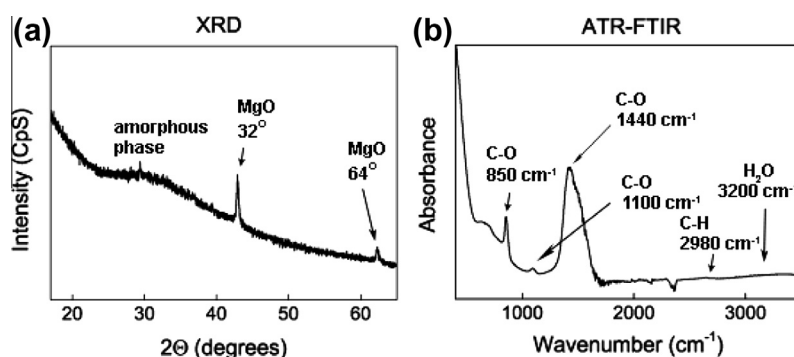
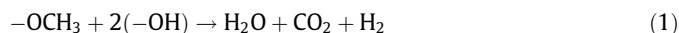


Fig. 2. Characterization of the three months stored Upsalite, (a) X-ray diffractogram, peaks stem from remaining crystalline magnesium oxide. A broad halo at 20 – 30° indicates the presence of at least one amorphous phase. (b) ATR-FTIR spectrum, the peaks correspond to C–O vibration from the carbonate.

spectrum displayed small peaks centered around 2980 cm⁻¹ corresponding to C–H vibrations. These peaks are more distinguishable in the previously presented as-synthesized material [27] indicating that during the three months storage period some of the organic groups have decomposed. The presence of such peaks indicates that some methoxyl groups remain in the samples after synthesis and even after long-term storage in air at moderate temperatures. A weak, broad band centered around 3450 cm⁻¹ is also present in the spectrum stemming from hydroxyl groups [32] likely formed due to adsorption of water on the surface of the material. However, these hydroxyl groups may also be part of the material itself, as indicated by the presence of water above 250 °C in the EGA analysis described below. XRD and FTIR analyses of the samples after the different employed storage conditions show that the main chemical composition of the material remains unchanged, and that the material does not crystallize even upon calcination at 300 °C. The presence of methoxyl and hydroxyl groups in the uncalcined samples was also evident from the EGA analysis as the decomposition products water and carbon dioxide were detected in a temperature interval from slightly below 100 °C up to 250 °C, Fig. 3. These products are formed according to the following reaction [33]:



H₂ was not detected in the analysis due to its IR invisibility. The magnesium carbonate does not decompose below 300 °C as evident by the limited evolution of carbon dioxide at lower temperatures, Fig. 3.

As described earlier [27], the reaction between magnesium oxide, methanol and carbon dioxide results in the formation of an amorphous magnesium carbonate according to the reaction scheme below. The reaction scheme was discussed in our previously published article where the IR spectra of the first intermediate, Mg(OCH₃)(OH), was presented. It was further discussed that during the mild temperature and pressure conditions employed

for the reaction of Upsalite, a reaction between MgO and CO₂ without the presence of alcohol does not occur.

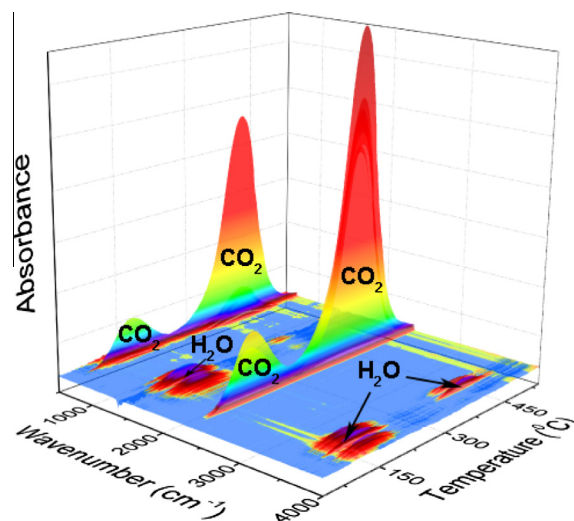
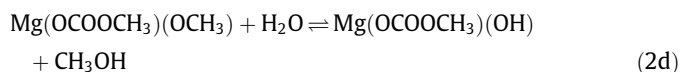
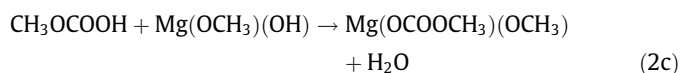
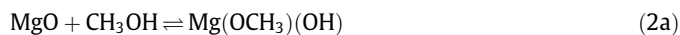
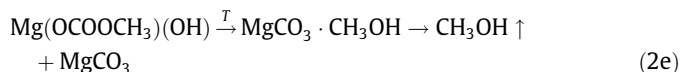


Fig. 3. EGA spectrum showing the decomposition products of the sample as a function of temperature.



The intermediate product $\text{Mg}(\text{OCOOCH}_3)(\text{OCH}_3)$ has earlier been shown to be able to physically bind carbon dioxide [28,34], which inevitably expands when leaving the material (in gas form) when the gel solidifies during heating at 70 °C in reaction step 2e. At the same time the intermediate product $\text{Mg}(\text{OCOOCH}_3)(\text{OH})$, via reaction 2d and 2e, is degraded to methanol and magnesium carbonate. The release of physically bound carbon dioxide from the gel upon solidification was visibly observed as the gel volume increased significantly when the pressure was released and the gel heated. Hence, the release of physically bound carbon dioxide and the evaporation of methanol from the gel most likely constitute the pore-forming processes in the material. However, as will be discussed below, reaction 2e does not reach full completion at 70 °C, leaving residual methoxyl and hydroxyl groups in the sample. When these are released upon calcinations, carbon dioxide and water are formed according to reaction 1.

Fig. 4a displays the N_2 sorption isotherm for the as-synthesized Upsalite, which exhibits a typical Type 1 shape according to the IUPAC classification and is indicative of a microporous material [35]. The pore size distribution obtained with the DFT method gave two maxima at 1.5 and 2.5 nm, respectively, Fig. 5. The material is, thus, essentially microporous with marginally smaller pores than the earlier presented material that was allowed to dry one day longer than the presently investigated sample [27], which is consistent with the observed loss of organic groups from the material. The SSA, pore volume and pore size of the material after the employed storage conditions are summarized in Table 1.

From the results summarized in Table 1 it is clear that the swelling of the gel due to expanding CO_2 gas and CH_3OH vapor in the solidification step is an irreversible event that causes formation of pores in the finally solid material. Interestingly, the pores do

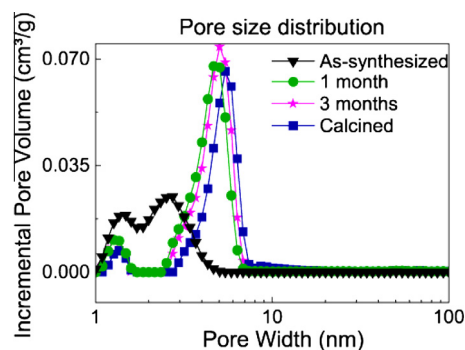


Fig. 5. Pore size distributions for Upsalite after synthesis (black triangles), 1 month storage (green circles), 3 months storage (pink stars) and calcined at 300 °C (blue squares). (For interpretation of the references to colour in this figure legend, the reader is referred to the web version of this article.)

not collapse during evaporation of the solvent, which otherwise could be expected, especially since an earlier study on the synthesis of porous magnesium carbonate in methanolic suspensions by Kornprobst and Plank showed that supercritical drying is needed to produce a porous material [28]. In their study the intermediate product $\text{Mg}(\text{OCOOCH}_3)(\text{OCH}_3)$ in methanol was hydrolyzed with water (2-fold excess with respect to solid content) in order to form a gel of magnesium carbonate that later was supercritically dried to form a porous material. This material, however, was composed of discrete amorphous nanoparticles assembled into a superstructure with an interparticulate pore network with pore sizes throughout the entire mesoporous range with a maximum around 15 nm. This contrasts largely to the air-dried Upsalite which is not composed of individual particles but rather maintains a continuous gel-like matrix structure [27] with a narrow pore size distribution.

After being stored in air at 70 °C for up to three months, a clear shift in pore size distribution for the current material towards the

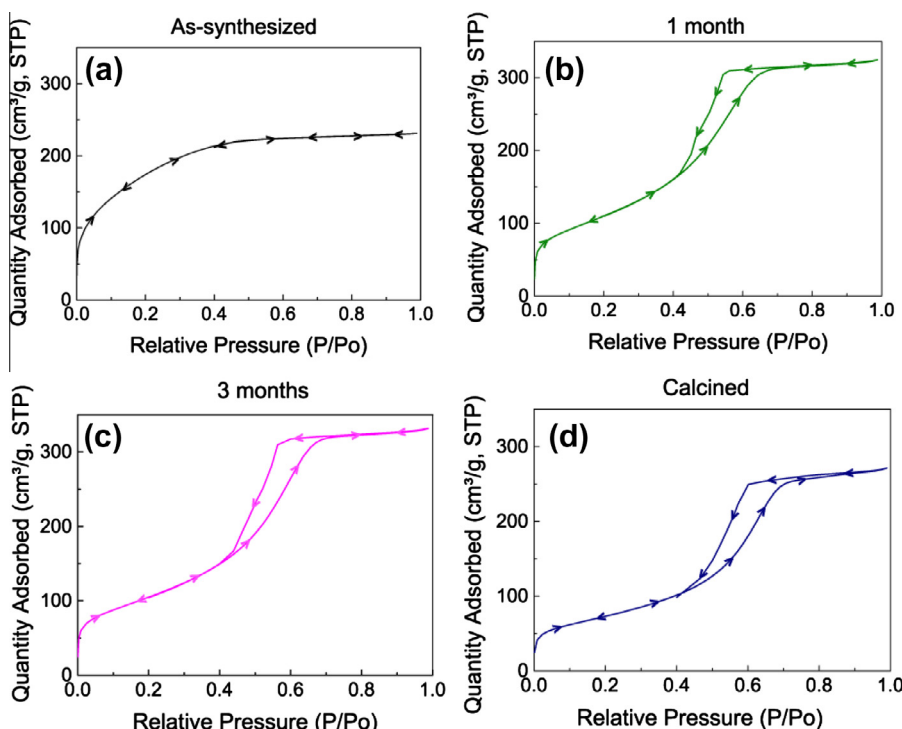


Fig. 4. Nitrogen sorption isotherms for Upsalite (a) as-synthesized, (b) after one month storage in air at 70 °C, (c) after three months storage in air at 70 °C and (d) calcined at 300 °C in a nitrogen atmosphere. Arrows indicate the direction of the relative pressure change.

Table 1
Specific surface area, pore volume and pore sizes for Upsalite after different storage conditions.

Sample	As-synthesized	1 month 70 °C air	3 months 70 °C air	Calcined 300 °C N ₂
SSA [m ² /g] ^a	638 ± 5	397 ± 3	387 ± 2	265 ± 1
Total pore volume [cm ³ /g] ^b	0.36	0.50	0.51	0.42
DFT pore width [nm] ^c	2.5	4.7	5.0	5.5
Limiting micropore volume [cm ³ /g] ^d	0.21 ± 0.00	0.13 ± 0.00	0.13 ± 0.00	0.10 ± 0.00

^a Established with the BET equation [29].

^b Single point adsorption at $P/P_0 \approx 1$.

^c Established by DFT analysis of the nitrogen adsorption isotherm.

^d According to the D–A equation [30], the divergence for all the values are less than 0.001.

mesoporous size range as compared to the as-synthesized sample was observed, Fig. 5. This shift was associated with a simultaneous decrease in SSA and an increase in pore volume, Table 1, explained by a decomposition of methoxyl and hydroxyl groups in the material according to reaction 1 since reaction 2e does not reach immediate completion at 70 °C. This is supported by the EGA analysis presented in Fig. 3, showing that there are organic groups remaining also in the sample stored for three months. Compared with the as-synthesized material two additional months of storage in air at 70 °C had only marginal effects on the evolution of the pore-size distribution and no detectable effect on the pore volume, Fig. 5 and Table 1. This suggests that the material equilibrates after about one month of storage and that higher temperatures are needed to remove the remaining surface groups as supported by the EGA data in Fig. 3. Calcination of the material led to reduction of the pore volume accompanied with a decrease in surface area and a slight shift of the pore size distribution towards larger pores. The reason for this reduction in pore volume is not clear but it might be due to Ostwald ripening of the pores since the higher temperature increases the mobility of the constituents of the material.

It was earlier verified that the as-synthesized amorphous Upsalite does not crystallize even after at least 11 weeks of storage in an atmosphere saturated with water vapor [27]. However, when the calcined material was subjected to the same storage conditions it crystallized within two weeks to form nesquehonite (Mg(HCO₃)(OH)·2H₂O) as evident from the XRD pattern in Fig. 6. Yet, the water-induced transformation into nesquehonite was slow and when the material was stored for only two days at 100% RH, virtually all adsorbed water could be removed by subsequent heat-treatment at 250 °C, as verified by a comparison of the weight of the dry, and the water saturated and thereafter dried sample. The above findings indicate that the organic surface groups present in the non-calcined material protect the bulk material from water molecules that otherwise may cause crystallization upon prolonged exposure to humidity.

From the presented results it may be concluded that the pores in Upsalite are formed via two mechanisms, illustrated in Fig. 7:

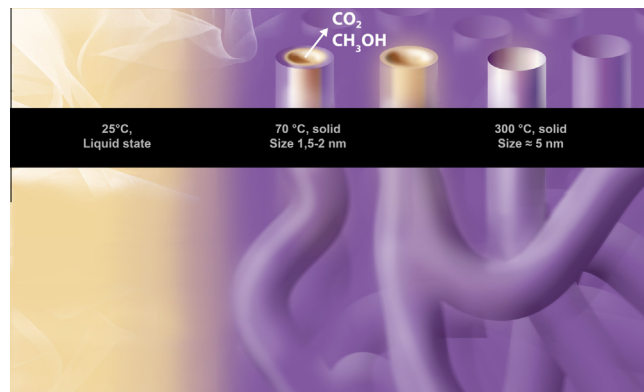


Fig. 7. Schematic description of the pore formation mechanism in Upsalite starting from the liquid state (left) from which micropores are formed due to solvent evaporation and CO₂ gas release. The micropores expand into mesopores when stored in air at 70 °C due to continual removal of organic groups remaining in the material. Upon calcination at temperatures above 250 °C (here 300 °C) all the organic groups are removed from the material, as shown in the right hand-side of the illustration.

1. First a rapid evolution of expanding carbon dioxide gas occurs together with methanol evaporation during solidification of the gel; the gel is rigid enough during the transition into a solid material to inhibit collapse of the pores. Together these two events form the initially microporous material.
2. Upon storage in air at elevated temperatures below 100 °C (70 °C specifically studied), a *partial* decomposition of methoxyl and hydroxyl groups occurs causing augmentation of the micropores accompanied with an increase in total pore volume and decrease in the specific surface area. Calcination of the material at elevated temperatures above 250 °C (300 °C specifically studied) results in a *complete* removal of methoxyl and hydroxyl groups and densification and/or pore ripening.

4. Summary and conclusions

A detailed study of the pore forming mechanism as well as the stability of the high-surface area magnesium carbonate Upsalite has been performed. The pores in Upsalite were found to be formed in a two-step process where the first includes the formation of micropores by the release of expanding physically bound carbon dioxide and solvent evaporation. Storage of the microporous material in air at temperatures below 100 °C leads to pore-size augmentation due to partial decomposition of organic groups on the surface of the pore walls. The resulting material has a narrow pore size distribution centered at 5 nm and the stability of the amorphous structure in a humid atmosphere remains. Upon calcination at temperatures above 250 °C, the organic groups are completely removed from the material. After this removal the material is able to bind water in its structure which crystallizes into nesquehonite

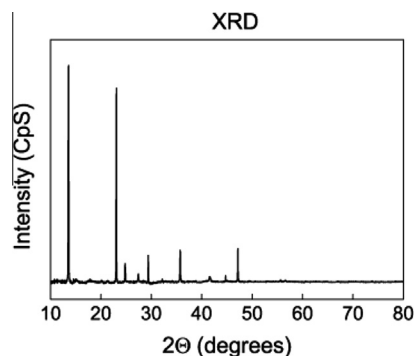


Fig. 6. XRD pattern for the calcined sample stored in a humid atmosphere, the peaks correspond to nesquehonite (MgCO₃(OH)·2H₂O).

when stored in a humid atmosphere for a time period longer than one week, prior to that no crystallization occurs. The results presented herein further suggest that it might be possible to control the pore size of the material via moderate heat treatments. Whereas very recent work analyses the dielectric response of water in the studied material [36], future studies will focus on applications in drug delivery.

Acknowledgments

Associate Professor Muhammet Toprak and Dr Xiadai Wang at the Royal Institute of Technology (KTH) in Stockholm are greatly acknowledged for the assistance in the EGA analysis. Dr. Alfonso Garcia-Bennett at Stockholm University is greatly acknowledged for recording the TEM image and Christoffer Karlsson at Uppsala University is greatly acknowledged for assistance with the EGA data plot. The Swedish funding agency VINNOVA and the Carl Trygger Foundation are gratefully acknowledged for funding this work.

References

- [1] G.Q. Lu, X.S. Zhao, *Nanoporous Materials – Science and Engineering*, World Scientific, Secondary, 2004.
- [2] F. Hoffmann, M. Cornelius, J. Morell, M. Fröba, *Angew. Chem. Int. Edit.* 45 (2006) 3216–3251.
- [3] M.E. Davis, *Nature* 417 (2002) 813–821.
- [4] A. Corma, *Chem. Rev.* 97 (1997) 2373–2420.
- [5] A. Sayari, *Chem. Mater.* 8 (1996) 1840–1852.
- [6] J.Y. Ying, C.P. Mehnert, M.S. Wong, *Angew. Chem. Int. Edit.* 38 (1999) 56–77.
- [7] B. Fadeel, B. Kasemo, M. Malmsten, M. Strømme, *J. Intern. Med.* 267 (2010) 2–8.
- [8] M. Vallet-Regí, *J. Intern. Med.* 267 (2010) 22–43.
- [9] H. Vallhov, N. Kupferschmidt, S. Gabrielsson, S. Paulie, M. Strømme, A.E. Garcia-Bennett, A. Scheynius, *Small* 8 (2012) 2116–2124.
- [10] H. Vallhov, S. Gabrielsson, M. Strømme, A. Scheynius, A.E. Garcia-Bennett, *Nano. Lett.* 7 (2007) 3576–3582.
- [11] U. Brohede, R. Atluri, A.E. Garcia-Bennett, M. Strømme, *Curr. Drug Deliv.* 5 (2008) 177–185.
- [12] M. Strømme, U. Brohede, R. Atluri, A.E. Garcia-Bennett, *Wiley Interdiscip Rev Nanomed Nanobiotechnol* 1 (2009) 140–148.
- [13] A. Mihranyan, N. Ferraz, M. Strømme, *Prog. Mater. Sci.* 57 (2012) 875–910.
- [14] C.T. Kresge, M.E. Leonowicz, W.J. Roth, J.C. Vartuli, J.S. Beck, *Nature* 359 (1992) 710–712.
- [15] J.S. Beck, J.C. Vartuli, W.J. Roth, M.E. Leonowicz, C.T. Kresge, K.D. Schmitt, C.T.-W. Chu, D.H. Olson, E.W. Sheppard, S.B. McCullen, J.B. Higgins, *J. Am. Chem. Soc.* (1992) 10834–10843.
- [16] S. Inagaki, Y. Fukushima, K. Kuroda, *J. Chem. Soc. Chem. Comm.* 8 (1993) 680–682.
- [17] S. Inagaki, A. Koiwai, N. Suzuki, Y. Fukushima, K. Kuroda, *Bull. Chem. Soc. Jpn.* 69 (1996) 1449–1457.
- [18] R. Atluri, N. Hedin, A.E. Garcia-Bennett, *J. Am. Chem. Soc.* 131 (2009) 3189–3191.
- [19] A.E. Garcia-Bennett, *Nanomedicine* 6 (2011) 867–877.
- [20] A.E. Wan, Zhao, *Chem. Rev.* 107 (2007) 2821–2860.
- [21] R. Ryoo, J.M. Kim, C.H. Ko, C. Shin, *J. Phys. Chem.* 100 (1996) 17718–17721.
- [22] L. Baù, B. Bártová, M. Arduini, F. Mancin, *Chem. Commun.* (2009) 7584–7586.
- [23] M.E. Davis, *Chem. Eur. J.* 3 (1997) 1745–1750.
- [24] L.-H. Chen, X.-Y. Li, G. Tian, Y. Li, J.C. Rooke, G.-S. Zhu, S.-L. Qiu, X.-Y. Yang, B.-L. Su *Angew. Chem. Int. Edit* 50 (2011) 11156–11161.
- [25] J. Jiang, J. Yu, A. Corma, *Angew. Chem. Int. Edit* 49 (2010) 3120–3145.
- [26] J. Forsgren, M. Andersson, P. Nilsson, A. Mihranyan, *Adv. Healthcare Mater.* 2 (2013) 1469–1476.
- [27] J. Forsgren, S. Frykstrand, K. Grandfield, A. Mihranyan, M. Strømme, *PLoS ONE* 8 (2013) e68486.
- [28] T. Kornprobst, J. Plank, *J. Non-Cryst Solids* 361 (2013) 100–105.
- [29] S. Brunauer, P.H. Emmett, E. Teller, *J. Am. Chem. Soc.* 60 (1938) 309–319.
- [30] M.M. Dubinin, V.A. Astakhov, Description of Adsorption Equilibria of Vapors on Zeolites over Wide Ranges of Temperature and Pressure, *Molecular Sieve Zeolites-II*, American Chemical Society, Washington D.C., 1971, pp. 69–85.
- [31] G. Raade, *Am. Mineral* 55 (1970) 1457–1465.
- [32] Y. Diao, W.P. Walawender, C.M. Sorensen, K.J. Klabunde, T. Ricker, *Chem. Mater.* 14 (2002) 362–368.
- [33] J. Suuronen, I. Pitkänen, H. Halttunen, R. Moilanen, *J. Therm. Anal. Calorim.* 69 (2002) 359–369.
- [34] H.L. Finkbeiner, M. Stiles, *J. Am. Chem. Soc.* 85 (1963) 616–622.
- [35] K.S.W. Sing, D.H. Everett, R.A.W. Haul, L. Moscou, R.A. Pierotti, J. Rouquerol, T. Siemieniowska, *Pure Appl. Chem.* 57 (1985) 603–619.
- [36] I. Pochard, S. Frykstrand, O. Ahlström, J. Forsgren, M. Strømme, *J. Appl. Phys.* 115 (2014) 044306.